

# Monitoring Natural Vegetation in Southern Greenland Using NOAA AVHRR and Field Measurements

BIRGER ULF HANSEN<sup>1</sup>

(Received 6 June 1990; accepted in revised form 5 June 1991)

**ABSTRACT.** The application of the Normalized Difference Vegetation Index (NDVI) for monitoring natural vegetation and biomass production has been evaluated for a sheep farming area in southern Greenland. Field measurements of spectral reflectance data during the growing season have been used to make a calibration between NOAA AVHRR NDVIs and aboveground vegetation quantities. The potential biomass production is estimated as the product of mean NDVI and the length of the growing season. Lowest-order atmospheric as well as geometric corrections were carried out on the satellite data before the seasonal and regional variations were correlated with climate and water balance.

Agriculture in southern Greenland started when Eric the Red came from Iceland around 982 A.D., and the Norse era ended approximately 500 years later because of climatic change, extensive overgrazing and soil erosion. Modern sheep farming started in 1924, but the threats to sheep breeding and the environment are the same today as during the Norse era.

The satellite-based monitoring has proved to be a useful tool to avoid overgrazing, which in this foehn-affected area easily implies soil erosion. It is a quick and low-cost method, and in combination with meteorological and soil water data it is possible to forecast the dry biomass production at the beginning of each growing season. This facilitates agricultural management and planning of the potential breeding capacity in this vulnerable marginal environment.

**Key words:** southern Greenland, NOAA-AVHRR, Normalized Difference Vegetation Index, atmospheric corrections, biomass production

**RÉSUMÉ.** On a évalué l'application de l'indice de végétation par différence normalisée (NDVI) pour surveiller la production de végétation naturelle et de biomasse dans une région d'élevage ovin au sud du Groenland. On a utilisé les mesures prises sur le terrain des données du facteur de réflexion spectrale au cours de la saison de croissance pour établir un étalonnage entre les NDVI obtenus au radiomètre perfectionné à très haute résolution de la NOAA et les quantités de végétation au-dessus du sol. L'évaluation de la production potentielle de biomasse correspond au produit de la moyenne du NDVI et de la durée de la saison de croissance. On a effectué sur les données par satellite des corrections atmosphériques et géométriques de l'ordre le plus faible, avant d'établir la corrélation entre les variations saisonnières et régionales d'une part et le climat et le bilan hydrique d'autre part.

Les débuts de l'agriculture dans le Groenland méridional coïncident avec la venue d'Islande d'Erik le Rouge aux alentours de l'an 982 de notre ère; environ 500 ans plus tard, un changement dans le climat, la surexploitation des pâturages et l'érosion du sol signalèrent la fin de l'époque scandinave. En 1924 débuta l'élevage ovin moderne, mais les menaces qui pèsent sur lui et sur l'environnement sont les mêmes aujourd'hui qu'au temps des Scandinaves.

La surveillance par satellite s'est révélée être un outil efficace pour prévenir la surexploitation des pâturages, qui, dans cette région affectée par le foehn, équivaut vite à une érosion du sol. C'est une méthode rapide et peu coûteuse qui, combinée avec les données météorologiques et les données hydriques du sol, permet de prévoir la production de biomasse sèche au début de chaque saison de croissance. La gestion de l'agriculture en est facilitée de même que la planification de la capacité potentielle d'élevage dans cet environnement caractérisé par sa vulnérabilité.

**Mots clés:** Groenland méridional, radiomètre perfectionné à très haute résolution de la NOAA, indice de la végétation par différence normalisée, corrections atmosphériques, production de biomasse

Traduit pour le journal par Nésida Loyer.

## INTRODUCTION

The first period with agriculture in southern Greenland started when Eric the Red came from Iceland around 982 A.D. Five hundred years later the Norse era came to an end because of climatic change, extensive overgrazing and soil erosion (Jakobsen, 1990). The second period began in 1924, when the first modern full-time sheep breeder started at Qagssiarssuk (Fig. 1), close to the ruin of Eric the Red's farm. Today 60-70 families have sheep breeding as their chief occupation, with 40 000 sheep on grass during the summer and 20 000 in stables in winter; the main sheep breeding is located in the sub-alpine central region between Upernaviarssuk, Qagssiarssuk and Sdr. Igaliko. In the two periods of agricultural land use in southern Greenland the basis has been grazing of the natural vegetation and stall feeding with hay produced within the area.

The impact on landscape and vegetation is heavy and probably irreversible in some areas due to the fact that plant production is very sensitive to even minor climatic fluctuations. Recent soil studies (Jakobsen, 1990) and pollen studies (Fredskild, 1988) have shown that several areas already suffer from overgrazing and various stages of soil erosion can be seen. The studies also show significant soil erosion during the Norse era. Data from the advanced very high resolution

radiometer (AVHRR) aboard the National Oceanic and Atmospheric Administration's (NOAA) satellite have been

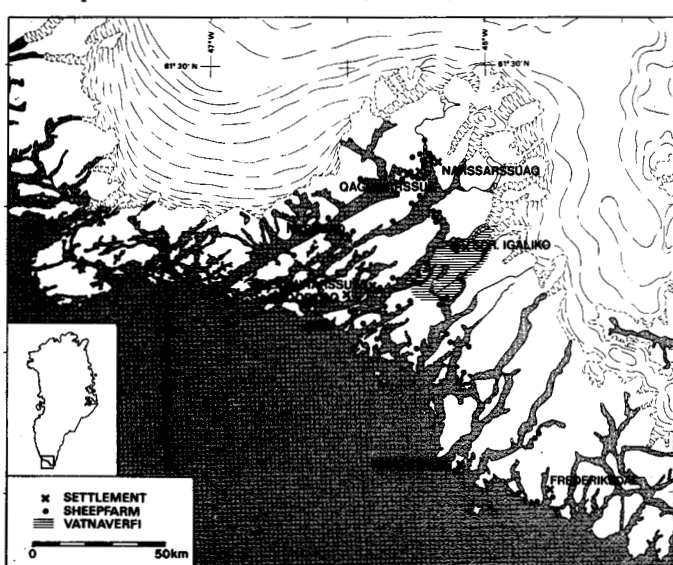


FIG. 1. The sheep-breeding district in southern Greenland. Most sheep farms are located close to ruins from the Norse era.

<sup>1</sup>Institute of Geography, University of Copenhagen, Øster Voldgade 10, DK-1350 Copenhagen K, Denmark  
© The Arctic Institute of North America

used to calculate vegetation indices, which were used to estimate the actual local breeding capacity and to procure a planning tool for the future growth of the sheep stock. The method can be used to follow the regional variation of the vegetation within a growing season and also to detect changes from year to year.

#### THE STUDY AREA

The area belongs to the arctic/subarctic marginal zone and is characterized by deep fjords nearly reaching the alpine border area of the ice cap. The climate is exposed to the interaction between the polar air mass from the ice cap and the maritime air from the ocean, which results in abrupt changes in the meteorological parameters. Due to the maritime influence, the mean July temperature at sea level increases from 5-6°C at Qaqortoq at the outer coast to around 9-10°C at the more continental located Narssarssuaq. The mean annual temperature in Narssarssuaq is 1.0°C, with a yearly variation of 17°C (Fig. 2). The temperature amplitude is smaller at the coast, and the low temperatures occur partly because of the proximity of the polar ice drift. This ice causes frequent foggy conditions all along the outer coast of south Greenland.

The mean annual precipitation is highest in the coastal area, with 820 mm at Qaqortoq, and decreases to 600 mm at Narssarssuaq. Roughly 50% of the precipitation falls in the growing season (May-September), as seen on Figure 3. In warm and very dry summers only 110 mm of precipitation falls in the inner parts of the region (Fig. 3), compared to 170 mm in the coastal areas. The daily evapotranspiration is 1-3 mm, and the annual evapotranspiration increases from 150 mm in the coastal areas to 300 mm farther inland.

In the valleys of the central region most soils show a field capacity of 50-150 mm at the beginning of the growing season. The soil water balance during the growing season is primarily influenced by the frequent occurrences of a strong, dry

foehn wind, which may occur 6-7 times during the summer. As these may result in a daily evapotranspiration of 16 mm/day, there is, in dry periods, risk of drought on valley sides with low field capacity, and consequently low dry-matter production.

Most of the high inland area towards the ice cap and a narrow coastal zone are barren, except for lichen vegetation. For the rest of the region the vegetation is extremely well adapted to the climatic and topographical conditions. Fell-field vegetation is found on top of the windswept ridges, stony barrens and stony terraces. Grassland is common on slopes well protected by a not long-lived snow cover during the winter. Wetland types such as fen and marsh are found as narrow zones along lakes and streams, while in the subarctic inner region thickets of birch and willow can be found in protected valleys. From the coastal areas the luxuriance of the vegetation increases inland, but larger homogeneous areas of vegetation are rare, whereas patchy heterogeneous plant communities between bare rocks are common.

#### SATELLITE DATA APPROACH

Due to the high latitude of the study area, Meteosat data cannot be applied, and the low orbital altitude of SPOT and Landsat 4/5 Thematic Mapper (TM) prevents the ground station at Kiruna, Sweden, from receiving direct data from these satellites. SPOT claims to provide worldwide data from the onboard recorders, but they have to be programmed before leaving the coverage area of the ground station and only a limited amount of data can be recorded on each orbit. During the last three years local low-budget projects have lost in competition with high-budget American/Canadian projects, and only two cloud-free scenes have been received.

Because of the close position to the major Atlantic cyclone track, southern Greenland experiences long periods of dense cloud cover, which favours the choice of NOAA-AVHRR data. The NOAA-AVHRR was designed as a meteorological instrument for detecting clouds and surface temperature over large areas. Channels 1 and 2 on the NOAA-AVHRR measure reflected solar radiation, while channels 3-5 are designed for infrared and thermal infrared radiation (Table 1).

During the last 10 years, these satellite data have been used for monitoring large areas of vegetation. The red band (chan-

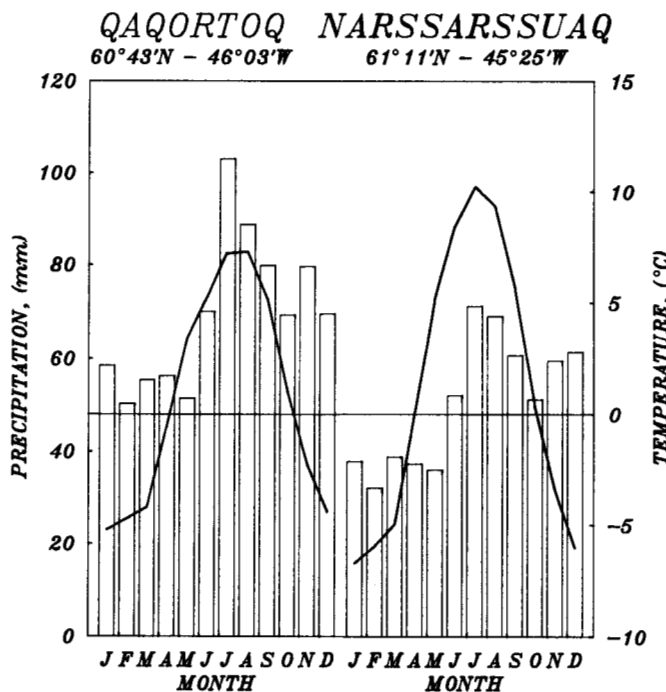


FIG. 2. Interannual variations in temperature and precipitation at Qaqortoq and Narssarssuaq.

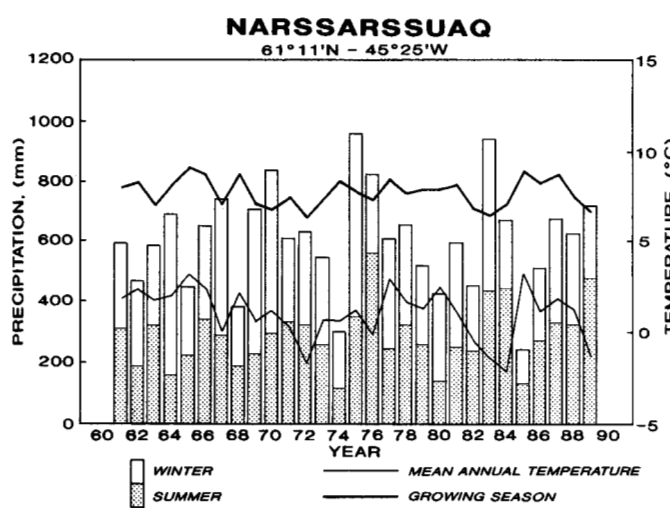


FIG. 3. Annual variation in temperature and precipitation at Narssarssuaq.

nel 1) of the AVHRR contains the chlorophyll absorption band (0.4-0.7  $\mu\text{m}$ ), while the reflection from the near-infrared band (channel 2) depends on the leaf area and leaf structure.

In order to minimize the unwanted effects on signals reaching the sensor, a commonly used dimensionless index derived from these data is known as the Normalized Difference Vegetation Index (NDVI) (Holben, 1986) and is defined as  $\text{NDVI} = (\text{A}_2 - \text{A}_1)/(\text{A}_2 + \text{A}_1)$ , where  $\text{A}_1$  and  $\text{A}_2$  are the reflectances measured in channel 1 and channel 2. However, it should be noted that using the ratio does not eliminate additive effects due to atmospheric attenuation. If AVHRR data are to be effectively applied it is important to take into account the effect of atmospheric scattering and absorption on sensor response due to off-nadir viewing of the instrument.

#### PROCESSING OF SATELLITE DATA AND ATMOSPHERIC CORRECTION

The image processing of the satellite data was made with the "CHIPS" system (Holm *et al.*, 1988), developed at the Institute of Geography, University of Copenhagen. Cloud-free scenes of the study area are rather rare, so to get the best time sampling every suitable scene must be used and hence corrected for atmospheric and geometrical effects. For correction of the latter, a systematic correction for the panoramic effect and a transformation to UTM-model by a cross-correlation technique were used to allow a high sub-pixel accuracy.

An automatic filtering procedure is used to remove sea-, snow-, cloud- and haze-contaminated pixels, which minimize later computing time. A combination of surface temperatures determined by the "split-window" technique (Hansen, 1989) and the surface albedo removes sea, snow and cloud pixels, while the difference between brightness temperatures in channels 4 and 5 with empirically determinated thresholds is used to remove pixels contaminated by haze and semi-transparent clouds. Using the split-window technique, only odd-numbered NOAA satellites with afternoon passes can be applied, because the 11.5-12.5  $\mu\text{m}$  band is not present on even-numbered satellites.

The AVHRR radiance values are a function of solar zenith angle, look zenith angle and the look azimuth, assuming constant atmospheric conditions. These angles describe AVHRR viewing and illumination geometry. Given the day number, ascending nodal time and longitude, satellite height, inclination angle and time of the scan line, it is possible to calculate longitude, latitude, local time and solar zenith angle for each pixel with a high degree of accuracy (Ho and Asem, 1986). As the solar zenith angle is a function of latitude, it changes approximately 20° across a scan line, while it changes approximately 45° between the summer and winter solstice. The look zenith angle varies in proportion to the scan angle, ranging from 0° at the nadir to ±68° for extreme off-nadir viewing. The look azimuth angle is necessary for computing the amount of scattering in the atmosphere. As the azimuth of the scan plane is constant for a given location and from orbit to orbit, the variation in the look azimuth angle depends only on the variation of the solar azimuth angle. For a latitude of 61° N and at the summer solstice, the variation of the look azimuth angle along a scan line is less than 10°. The difference between summer and winter ranges from approximately 0° in extreme forward scatter direction to approximately 20° in extreme backscatter direction. The constant look azimuth

angle at extreme forward scatter direction is due to a local solar time very close to noon (Hansen, 1990).

The atmospheric effect on the AVHRR albedos has been simulated with the SIMUSAT model developed at the Institute of Geography, University of Copenhagen (Hansen, 1990). The model is a further development of and combination of the ATMOS model (Singh, 1988) and the RAYLEIGH model (Phulpin *et al.*, 1989). The SIMUSAT model starts with the assumptions of a single scattering approximation, a unit scattering albedo, a horizontally homogeneous atmosphere, a Lambertian surface and a low aerosol mass loading, and it corrects for scattering (Rayleigh and aerosol) and gaseous absorption ( $\text{O}_3$  and  $\text{H}_2\text{O}$ ). The Rayleigh phase function is well known and the aerosol phase function was approximated by a simplified version of the Two Term Heyney-Greenstein (TTHG) function as given in Liou (1980). The amount of ozone was obtained as a function of latitude, longitude and day number (Bowman and Krueger, 1985), while the atmospheric water vapour content was derived as a function of the difference between brightness temperatures in channels 4 and 5 (Dalu, 1986; Hansen, 1989). The main advantage of the SIMUSAT model is that it can easily be inverted to give satellite-observed reflectance as a function of measured surface reflectance.

The model was tested using measured surface reflectance for four cover classes (Table 2). Bands of NDVI versus scan angles were constructed for summer solstice illumination geometry assuming a low aerosol mass loading (Fig. 4). The upper bounds were defined by no water vapour in the atmosphere and the lower bounds by 3 cm water vapour, which is approximately the maximum value observed during cloudless situations. The slope of the NDVI curves was least for scan angles at nadir or slightly in the forward scatter direction. The width of a band increased as the amount of green vegetation decreased or as the reflectance from near infrared (NIR) decreased, and the band also became increasingly convex as green leaf biomass increased. The change in NDVI was simulated as a function of precipitable water for the four cover classes (Fig. 5). Within common range of precipitable water (0-3 cm) NDVI for high biomass decreased by 0.05 NDVI-

TABLE 1. Band width for the channels on NOAA-AVHRR

Channel no.	Band width ( $\mu\text{m}$ )	Denomination
1	.56-.68	Visible (VIS)
2	.725-1.10	Near infrared (NIR)
3	3.55-3.93	Mid-infrared
4	10.3-11.3	Thermal infrared
5	11.5-12.5	Thermal infrared

TABLE 2. Input surface reflectance for the simulation model of various general cover classes in the study area

Cover class	Reflectance			Canopy cover %	Wet bio (tons/ha)	Dry bio (tons/ha)
	VIS	NIR	NDVI			
High biomass	0.06	0.40	0.739	80-100	8.0-9.0	2.5-3.5
Medium biomass	0.08	0.30	0.579	50-70	3.0-4.0	1.0-1.5
Low biomass	0.10	0.20	0.333	20-40	0.5-1.0	0.2-0.3
Bare soil	0.17	0.19	0.056	0-10	0.0-0.2	0.0-0.1

units, or by 7%, while NDVI for low biomass decreased by 0.07–0.08 NDVI-units, or by 20–25%. As solar zenith angle increases from summer solstice to equinox, the absorption of NIR increases due to water vapour, while the NDVI for all four cover classes decreases and the bands in Figure 4 get more convex and broader. In early spring and late autumn spuriously high NDVI values have been observed for areas where there is no photosynthetic activity. This has been termed the terminator effect (Holben, 1986), and these spurious NDVI values are associated with very low visible (VIS) and NIR values, owing to larger atmospheric scattering and absorption due to large solar zenith angles and very long path lengths. A limit for the solar zenith angle of 80° has been suggested by Holben (1986), but the results from the study area suggest that no photosynthetic active processes are taking place in the period when the daily solar zenith angle is higher than 70°.

#### FIELD MEASUREMENTS

During the growing seasons in 1987 and 1989 intensive radiometric and biomass production measurements were carried out. The surface values of VIS and NIR were measured and NDVI values were calculated by applying two hand-held Milton radiometers (Hansen, 1988, 1990). At most plots a 25.5 cm<sup>2</sup> area was clipped, but at plots with scrub a 1 m<sup>2</sup> area was clipped. Each sampling was dried at 115°C and subsequently weighed to estimate dry biomass per m<sup>2</sup>. Before clipping, the distribution of species and the percentage cover were estimated from a 10 × 10 point grid.

Figure 6 shows the relationship between ground-measured NDVI and total accumulated dry-matter production in August

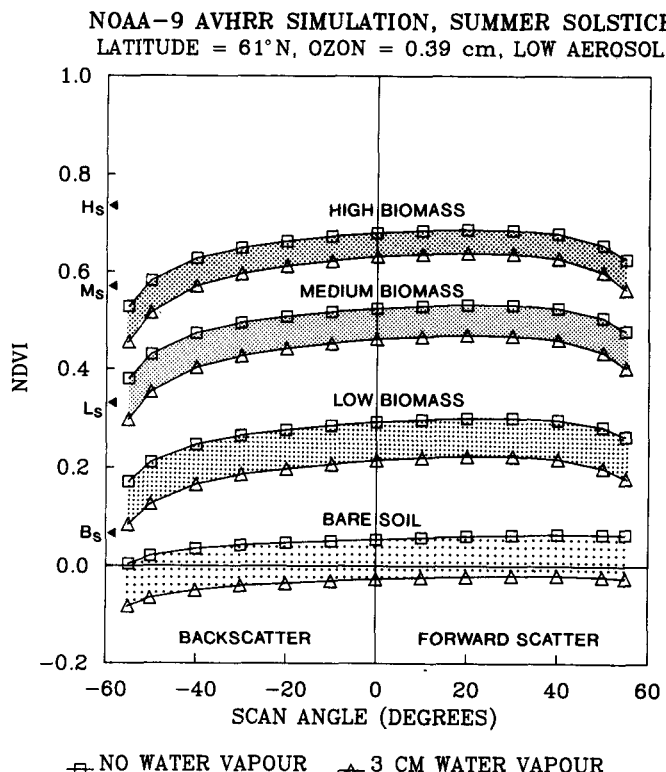


FIG. 4. The NDVI was simulated for AVHRR viewing and illumination conditions of the NOAA-9 afternoon equatorial crossing during the summer solstice. The simulation is shown as a function of scan angles for a range of cover types and different content of water vapour in the atmosphere.

1987 (Hansen, 1988), while Table 3 shows the wet and dry biomass production as a function of NDVI. More than 80% of the total variation can be explained by the hyperbolic curve, and there is no significant difference in seasonal variation of the slope of the curves. All surface cover types are represented; only chickweed (*Stellaria media*) is excluded from the calculations due to its extremely high water content and

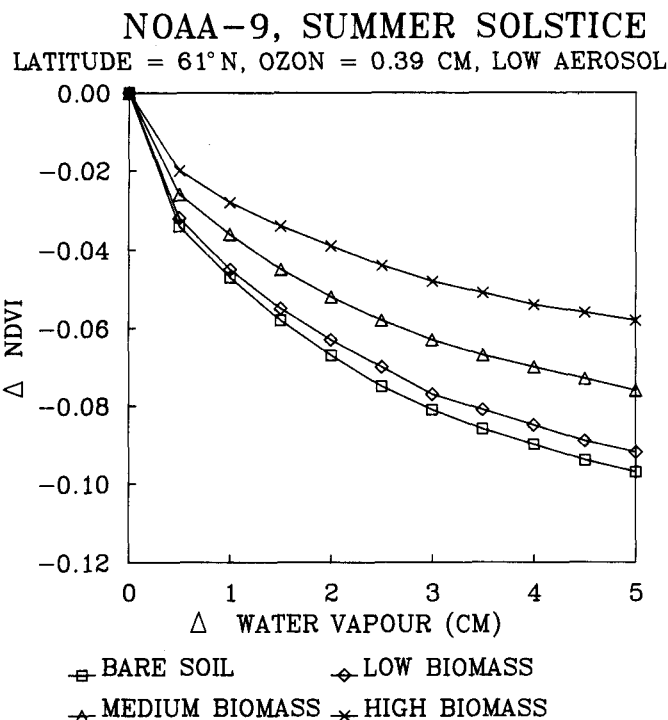


FIG. 5. The change in NDVI for a range of cover types as a function of precipitable water for NOAA-9 illumination during summer solstice at latitude 61°N.

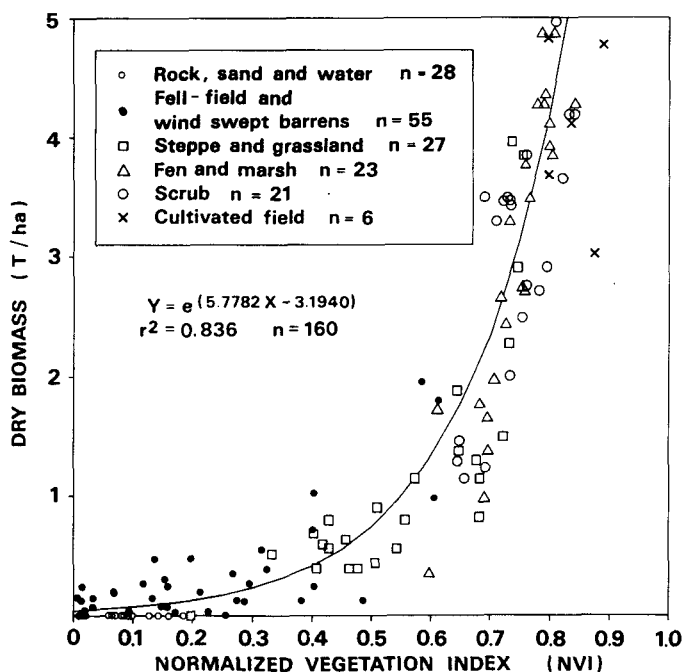


FIG. 6. The relationship between dry biomass production and NDVI at the optimum of the growing season in 1987.

TABLE 3. Wet and dry biomass production as a function of surface-estimated NDVI

Period	Biomass production (tons/ha)	n	R <sup>2</sup>
Aug-87	WET=exp[5.8717*NDVI-2.2797]	160	.885
Jun-89	WET=exp[5.6990*NDVI-2.1079]	105	.892
Aug-89	WET=exp[5.5889*NDVI-1.9335]	165	.867
Aug-87	DRY=exp[5.7782*NDVI-3.1940]	160	.836
Jun-89	DRY=exp[5.7134*NDVI-3.2602]	105	.870
Aug-89	DRY=exp[5.4884*NDVI-2.9359]	165	.840

because it has recently been imported and therefore is only found in small areas near the infields of the sheep farms. Normally, the dry biomass production varies between 30 and 50% of the wet biomass production.

During the growing season of 1989 the variation of VIS and NIR reflection was registered at 10 min intervals using a LICOR data logger. The variation in VIS reflectance was registered using LI-190SA Quantum Sensors (400-700 nm). A comparison with NOAA-AVHRR channel 1 reflectance is justified because the variation in the reflection within the photosynthetic active spectrum is very small. The NIR reflection was registered using LI-200SA Pyranometers (400-1100 nm) with a built-in 715 nm Schott-filter. Figure 7 shows the daily and seasonal variation of VIS, NIR reflectance and NDVI for a grassland slope well protected from grazing sheep. VIS reflectance decreases from 0.10 in the beginning of the field campaign to 0.06, while NIR reflectance started at 0.30 and had a maximum of approximately 0.45. NDVI started at zero just after the end of the snowmelt, and 14 days later it was 0.50. NDVI had a maximum of 0.80 in July and declined towards zero in the beginning of October. Unfortunately the growing season in 1989 was very cold and wet, so stress due to soil water deficit was not registered.

#### APPLICATION OF THE RESULTS

Frequent coverage of NDVI values during the growing season makes it possible to map several phytophenological parameters of importance for the vegetation. The onset and length of growing season are important parameters, which in arctic areas are controlled by the duration and magnitude of snow cover, while the time-integrated NDVI and maximum NDVI are controlled by precipitation, soil water storage, photosynthetic radiation and air temperature.

The regional variation of NDVI in 1987 is shown in Figure 8. Long duration and large magnitude of snow cover in the spring led to a shorter growing season and a smaller biomass production in the Vatnaverfi area, while several foehns and a small soil water storage at Akia implied stress on the vegetation in June and August and a low annual biomass production.

The annual variation of NDVI at Qagssiarssuk in 1985-89 is given in Figure 9. In 1985 the growing season started nearly 1.5 months before normal because of a very mild winter and spring. But each year maximum NDVI values fluctuated just below 0.3 at the end of July and the beginning of August, and from the beginning of September the NDVI diminished toward zero, which it reached in mid-October. No decline in NDVI due to soil water deficit was registered, mainly because

## GRASSLAND, 1989

TASIUSAQ, 61° 9'N – 45° 40'W

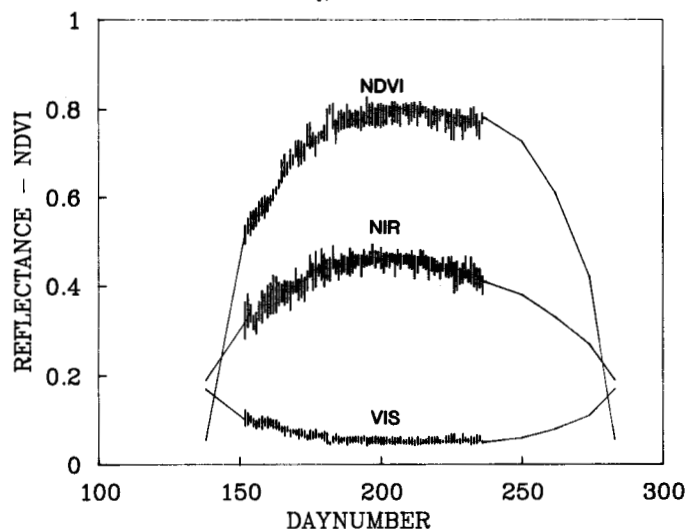


FIG. 7. The variation in VIS and NIR reflectance and NDVI for a grassland location during the growing season in 1989. Vertical lines indicate field measurements using surface radiometers (day number 150-239), while the rest of the curves are estimated from NOAA-satellite data.

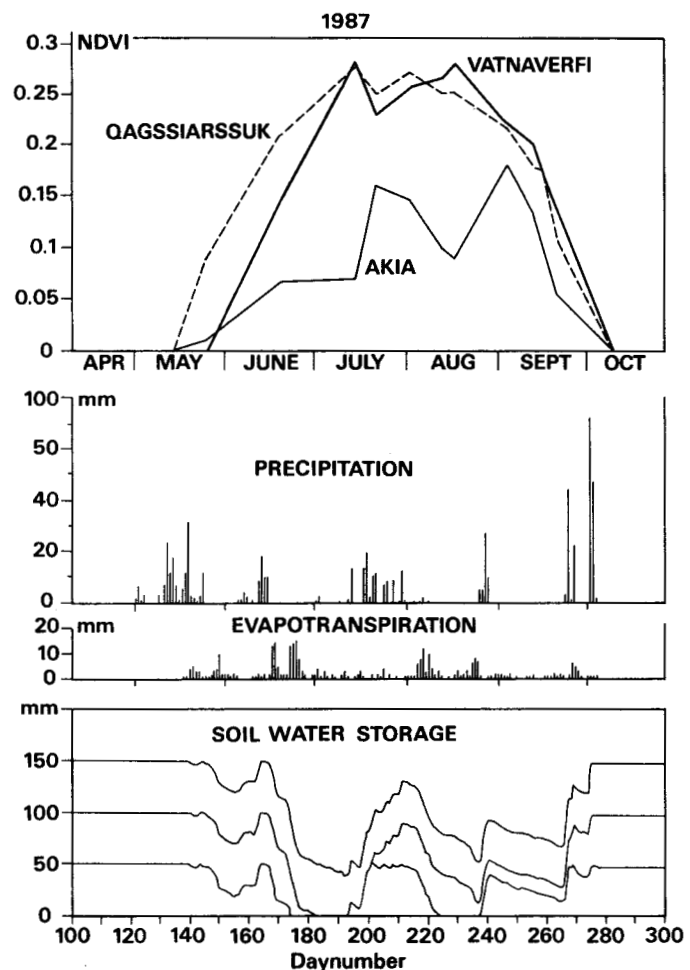


FIG. 8. Variation in NDVI for three locations during 1987 with daily values of evapotranspiration, soil water storage and precipitation from Upernviarssuk.

of the high soil water storage in the Qagssiarssuk area (100–150 mm). The NOAA-AVHRR-derived NDVIs are relatively

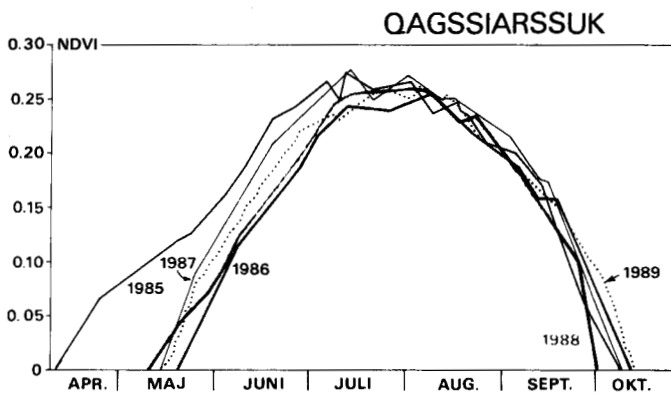


FIG. 9. Variation in NDVI throughout the growing seasons 1985-89 at Qagssiarssuk.

TABLE 4. Area ( $\text{km}^2$ ) for intervals of time-integrated NDVI values (iNDVI) in given altitude intervals (m asl) in 1989 (the total dry biomass production is calculated for the same intervals)

m asl	Total $\text{km}^2$	Area in $\text{km}^2$ for N = iNDVI										Dry bio (tons)
		N≤0	0<N≤5	5<N≤10	10<N≤15	15<N≤20	20<N≤25	25<N≤30	30<N≤35	35<N≤40		
0- 200	1302	231	164	148	163	209	240	142	5			66729
200- 400	776	176	111	71	81	111	143	82	2			37150
400- 600	666	259	112	71	93	76	53	3				18252
600- 800	604	393	106	57	32	13	3					5534
800-1000	552	442	84	21	5	1						1777
1000-1200	364	336	23	3	1							377
1200-1800	245	242	3									30
Total $\text{km}^2$	4508	2078	603	372	374	409	438	227	7			
Dry tons		0	6032	11166	18685	28630	39456	24970	910			129849

TABLE 5. The dry biomass production for the growing seasons 1985-89 for the total area and for luxuriant areas ( $i\text{NDVI} > 20$ )<sup>1</sup>

iNDVI	1985 $\text{km}^2$	Dry tons	1986 $\text{km}^2$	Dry tons	1987 $\text{km}^2$	Dry tons	1988 $\text{km}^2$	Dry tons	1989 $\text{km}^2$	Dry tons
$i\text{NDVI} \leq 0$	2760	0	2630	0	1921	0	2164	0	2709	0
$0 < i\text{NDVI} \leq 5$	1446	14460	1077	10770	1218	12180	1245	12450	1316	13160
$5 < i\text{NDVI} \leq 10$	716	21480	740	22200	790	23700	780	23400	683	20490
$10 < i\text{NDVI} \leq 15$	783	39150	893	44650	1027	51350	947	47350	823	41150
$15 < i\text{NDVI} \leq 20$	727	50890	986	69020	1179	82530	1035	72450	746	52220
$20 < i\text{NDVI} \leq 25$	382	34380	538	48420	725	65250	683	61470	627	56430
$25 < i\text{NDVI} \leq 30$	290	31900	282	31020	284	31240	276	30360	254	27940
$30 < i\text{NDVI} \leq 35$	59	7670	19	2470	21	2730	35	4550	7	910
$35 < i\text{NDVI} \leq 40$	2	300	0	0	0	0	0	0	0	0
Total	7165	200230	7165	228550	7165	268980	7165	252030	7165	212300
$i\text{NDVI} > 20$	733	74250	839	81910	1030	99220	994	96380	888	85280
DEM tons		22275		24573		29766		28914		25584
ECC sheep		44550		49146		59531		57828		51168
ACC sheep		36368		39237		39710		38775		37344
SWS kg		38.4		36.8		35.2		36.4		35.7

<sup>1</sup>The dry eatable matter production (DEM) is calculated as 30% of the dry biomass production in the luxuriant areas. The estimated carrying capacity (ECC) is calculated by assuming that the annual consumption rate per sheep is 500 kg DEM. The actual carrying capacity (ACC) and slaughter weight per sheep (SWS) are also shown for each year.

low, although high NDVI values can be found over small areas with high biomass production, but a NOAA pixel represents an area of 1  $\text{km}^2$  with a mixture of all surface cover types.

The integrated NDVI days during the growing season (iNDVI) is directly related to absorbed photosynthetically active radiation and hence total photosynthetic activity or productivity; this iNDVI from NOAA satellite data has proved to be a more precise estimator of the potential dry biomass production (P) at the end of the growing season (Tucker *et al.*, 1983). For the study area it is given by  $P(\text{kg/ha/year}) = 40 * i\text{NDVI}$ , which is similar to worldwide results (Goward *et al.*, 1985). For Qagssiarssuk the production can be estimated to 1160, 910, 1080, 960 and 1050 kg/ha for the period 1985-89 respectively. The variations during the last four years are mainly caused by variations in air temperature and in photosynthetic radiation.

A digital elevation model of a representative part of the area (63%) was used to calculate the variation in iNDVI in 1989 as a function of altitude. Table 4 shows that the most

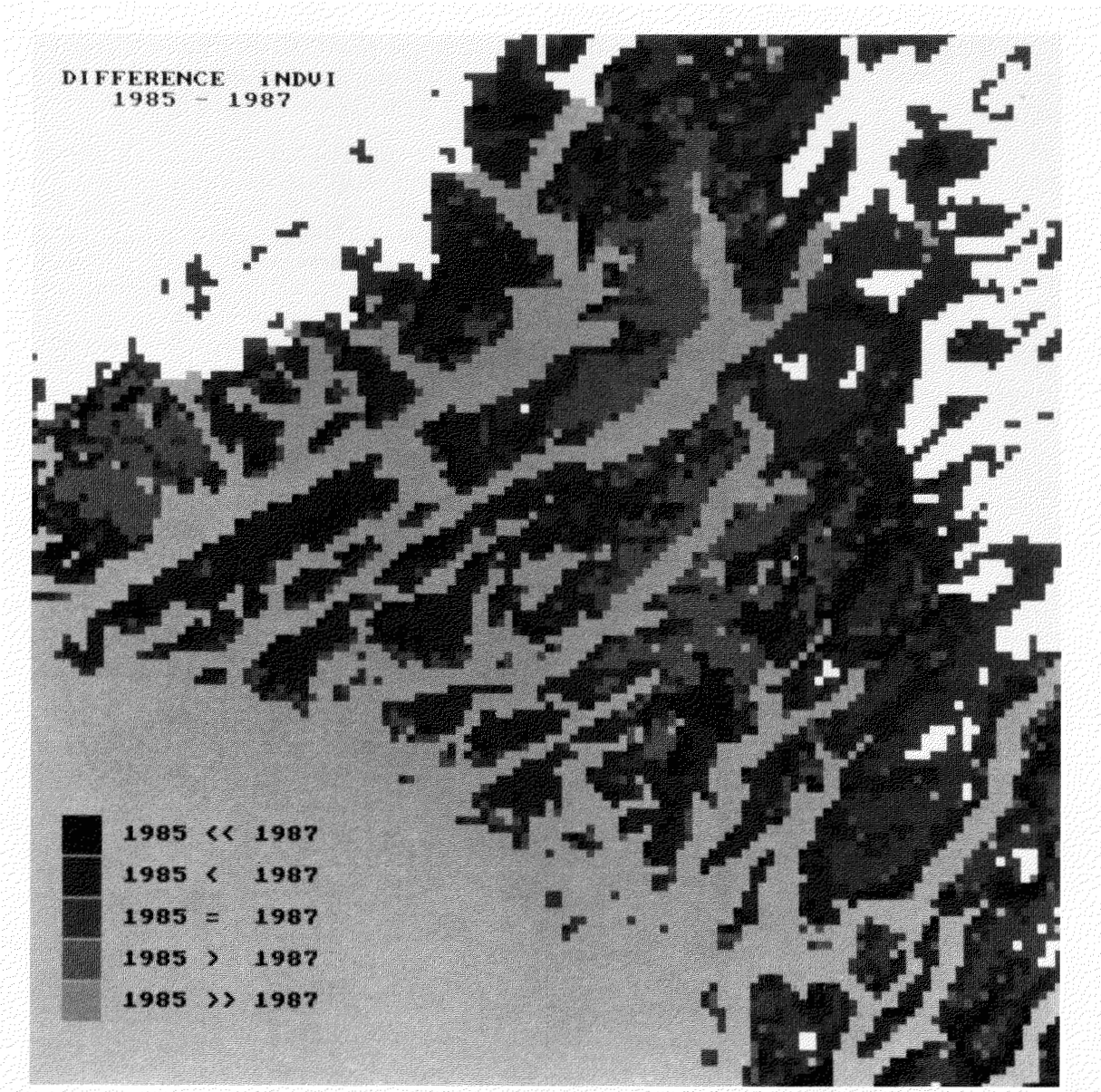


FIG. 10. Difference in dry biomass production between a very dry summer (1985) and a summer with a moderate and more evenly distributed precipitation (1987) (< indicates differences between 0 and 25%, while << indicates differences greater than 25%).

luxuriant areas ( $i\text{NDVI} > 20$ ) were placed within 0–600 m above sea level (asl). In 1989 they covered approximately 670 km<sup>2</sup>, or 15% of the area, and the dry biomass production in these luxuriant areas was about 65 000 tons, or 50% of the production in the total area. Nearly 1800 km<sup>2</sup>, or about 40% of the area, was placed above 600 m asl, and here the dry biomass production was only 7700 tons, or 6% of the production in the area covered by the digital elevation model.

The total dry biomass production for the entire sheep farming area in the years 1985–89 is given in Table 5. The dry biomass production was low in 1985, which was warm and dry, but low also in 1989, when the growing season was cold and precipitation was high. The dry biomass production was highest in 1987 and 1988, which were warm summers with moderate and more evenly distributed precipitation during the growing season. By comparing 1985 with 1987 (Fig. 10), it is evident that the higher soil water storage (100–150 mm) and the more continental climate at Qagssiarssuk and Vatnaverfi

result in high production in dry/warm summers, while the vegetation in the coastal areas and at higher altitudes is stressed due to a soil water deficit.

Knowing the dry biomass production of the total area, it is easy to calculate the carrying capacity. The calculations assume that only areas with  $i\text{NDVI} > 20$  are accessible or profitable for grazing. Unfortunately, sheep only use 30% of the dry-matter production, called DEM (dry eatable matter), and the annual consumption rate is 500 kg for each fertile ewe. Calculations of the optimal DEM production in 1985–89 and conversion to maximal carrying capacity show a 30% variation. For all years the actual carrying capacity is below the estimated maximal carrying capacity, but in 1985 these two figures were very close and a tendency toward overgrazing and soil erosion was seen in small areas with a concentration of farms, such as Qagssiarssuk, Igaliko and Vatnaverfi. As the actual carrying capacity is below the estimated carrying capacity, the slaughter weight per sheep is almost constant (36 kg)

during the five years, except in 1985, when the growing season was 1.5 months longer and the sheep were 2 kg fatter.

#### CONCLUSION

The satellite-based monitoring has proved to be a quick and low-cost method to register regional and seasonal variations in the natural vegetation, and in combination with meteorological and soil data it is possible to forecast the potential biomass production at the beginning of each growing season. This facilitates agricultural management and planning of the potential breeding capacity in this vulnerable marginal environment.

#### ACKNOWLEDGEMENTS

The project has kindly been supported by the Danish Natural Science Research Council, the Danish Commission for Scientific Research in Greenland and the Ministry for Greenland. The author wishes to thank Henrik Søgaard for reviews and valuable comments during the project and Henrik Steen Andersen and Jørgen Holm for programming aid. Further thanks go to Dr. Bent Fredskild, Jon Feilberg, Bjarne Holm Jakobsen, several students and local sheep farmers for valuable assistance during the field work.

#### REFERENCES

- BOWMAN, K.P., and KRUEGER, A.J. 1985. A global climatology of total ozone from the Nimbus 7 Total Ozone Mapping Spectrometer. *Journal of Geophysical Research* 90(D5):7967-7976.
- DALU, G. 1986. Satellite remote sensing of atmospheric water vapour. *International Journal of Remote Sensing* 7(9):1089-1097.
- FREDSKILD, B. 1988. Agriculture in a marginal area — south Greenland from the Norse Landnam (985 A.D.) to present (1985 A.D.). In: Birks, H.H., Birks, H.J.B., Kaland, P.E., and Moe, D. *The cultural landscape — past, present and future*. London: Cambridge University Press. 381-393.
- GOWARD, S.N., TUCKER, C.J., and DYE, G.D. 1985. North American vegetation patterns observed with the NOAA-7 advanced very high resolution radiometer. *Vegetatio* 64:3-14.
- HANSEN, B.U. 1988. Satellite monitoring of the biomass production in southern Greenland. *Geografisk Tidsskrift* 88:94-99.
- \_\_\_\_\_. 1989. Monitoring AVHRR derived vegetation indices and biomass production in southern Greenland. *Proceedings of 4th AVHRR Data Users' Meeting, EUMETSAT, Rothenburg, F.R. Germany*, 5-8 September 1989. 137-140.
- \_\_\_\_\_. 1990. Climate and vegetation analyses in southern Greenland using NOAA-AVHRR satellite data and field measurements. Ph.D. thesis, Institute of Geography, University of Copenhagen. 125. In Danish.
- HO, D., and ASEML, A. 1986. NOAA AVHRR image referencing. *International Journal of Remote Sensing* 7(7):895-904.
- HOLBEN, B.N. 1986. Characteristics of maximum-value images from temporal AVHRR data. *International Journal of Remote Sensing* 7(11):1417-1434.
- HOLM, J., OLESEN, H.H., SANDHOLT, I., ANDERSEN, H.S., and RASMUSSEN, K. 1988. CHIPS user's guide, Vers. 2.0. Copenhagen: Institute of Geography, University of Copenhagen.
- JAKOBSEN, B.H. 1990. The effect of climatic change on farming and soil erosion in southern Greenland during the last thousand years. Paper presented at the International Conference on the Role of the Polar Regions in Global Change, 11-15 June 1990, University of Alaska, Fairbanks, Alaska.
- LIOU, K.-N. 1980. An introduction to atmospheric radiation. *International Geophysics Series* 26. London: Academic Press. p. 392.
- PHULPIN, T., JULLIEN, J.P., and LASSELIN, D. 1989. AVHRR data processing to study the surface canopies in temperate regions. *International Journal of Remote Sensing* 10(4-5):869-884.
- SINGH, S.M. 1988. Estimation of multiple reflection and lowest order adjacency effects on remotely sensed data. *International Journal of Remote Sensing* 9(9):1433-1450.
- TUCKER, C.J., VANPRAET, C., BOERWINKEL, E., and GASTON, A. 1983. Satellite remote sensing of total dry matter production in the Senegalese Sahel. *Remote Sensing of Environment* 13:461-474.